

The Fly's Eye Extremely High Energy Cosmic Ray Spectrum

D.J. Bird,¹ S.C. Corbato,³ H.Y. Dai,³ B.R. Dawson,² J.W. Elbert,³ B.L. Emerson,³ M.A. Huang,³ D.B. Kieda,³ M. Luo,³ S. Ko,³ C.G. Larsen,³ E.C. Loh,³ M.H. Salamon,³ J.D. Smith,³ P. Sokolsky,³ P. Sommers,³ J.K.K. Tang,³ S.B. Thomas³

¹Department of Physics, University of Illinois at Urbana-Champaign, Urbana, IL 61801
USA

²Department of Physics and Mathematical Physics, University of Adelaide, Adelaide,
South Australia 5001 Australia

³High Energy Astrophysics Institute, Department of Physics, University of Utah,
Salt Lake City UT 84112 USA

ABSTRACT

We present our latest results on the cosmic ray energy spectrum above 10^{17} eV observed by Fly's Eye in the stereo (FEI plus FEII) mode. Data between 11/86 to 7/92 are used for deriving the stereo spectrum. Tracks detected by both eyes can be well reconstructed and therefore have very good energy resolution. A clear break between 2×10^{18} to 5×10^{18} eV has been observed in the energy spectrum. The paper presents spectral slopes before and after the break and the normalizations.

1. INTRODUCTION

The search for new features in the energy spectrum is important for its impact on theories of the origin, acceleration and propagation of cosmic rays. Despite a 30 year effort by many groups (Nagano *et al* 1992, Lawrence *et al* 1991, Efimov *et al* 1991), many details of the energy spectrum above 10^{17} eV are still limited by statistics, systematics and resolution.

Contrasted with the conventional widely spaced ground array technique, the Fly's Eye is designed to collect the atmospheric nitrogen fluorescence light produced by air shower particles. It is the only detector capable of measuring the individual longitudinal shower profile, which allows a direct (essentially interaction model independent) estimation of the primary energy.

In this paper, we present the energy spectrum measured by the Fly's Eye detector operated in stereoscopic mode. This data has improved cosmic ray track geometry resolution as compared to single eye resolution. Since the shower profile is simultaneously measured by two detectors, constraints on the energy resolution are possible.

2. THE FLY'S EYE EXPERIMENT

The details of the Fly's Eye experiments have been described in an earlier paper (Battarusaitis *et al* 1985). Only a brief description will be given here. The Fly's Eye detector began full operation in 1981 at Dugway, Utah (40° N, 113° W, atmospheric depth 860 g cm^{-2}). The original detector, Fly's Eye I, consists of 67 spherical mirrors of 1.5 m diameter, each with 12 or 14 photomultipliers in the focal plane. The mirrors are arranged so that the entire night sky is imaged, with each phototube viewing a hexagonal region of the sky 5.5 degrees in diameter. In 1986 a second detector (Fly's Eye II) 3.4 km away came into full operation. Fly's Eye II consists of 36 mirrors of the same design. This detector only views the half of the night sky in the direction of Fly's Eye 1. Fly's Eye II can be operated as a standalone detector or in conjunction with Fly's Eye I for a stereo view of a subset of the air showers. In total, there are 880 photomultiplier tubes in Fly's Eye I and 464 tubes in Fly's Eye II.

Optical reflectivity and photomultiplier tube gains are monitored by a light pulser every operating night. The two eyes only operate on clear and moonless nights which results in a 10% duty factor at Dugway.

3. DATA ANALYSIS AND ENERGY RESOLUTION

The air shower reconstruction process falls into two major divisions: geometric reconstruction and shower profile reconstruction. When a shower is seen simultaneously by Fly's Eye I and II, a shower-detector plane for each detector can be determined and the intersection of those planes defines the shower trajectory. With planar stereo reconstruction, no timing information is needed except to distinguish between upward and downward going tracks. Given the track geometry, the EAS longitudinal size $N_e(x)$ is calculated via an iterative process to remove the contributions due to the direct and scattered Cerenkov beam. The residual photo-electrons (after the Cerenkov contribution is removed) result from the atmospheric scintillation process and therefore directly proportional to the charged particle size within the tube field of view. Various attenuation effects between source and detector such as ozone absorption, aerosol and Rayleigh scattering are taken into account. Finally, each resultant longitudinal shower profile is approximated by a Gaussian function and the total primary energy is integrated using the fitted parameters.

The best way to study the energy resolution is to compare the energy calculated independently by Fly's Eye I and Fly's Eye II for events registered by both eyes. Figure 1 shows histograms of the fractional energy discrepancy between

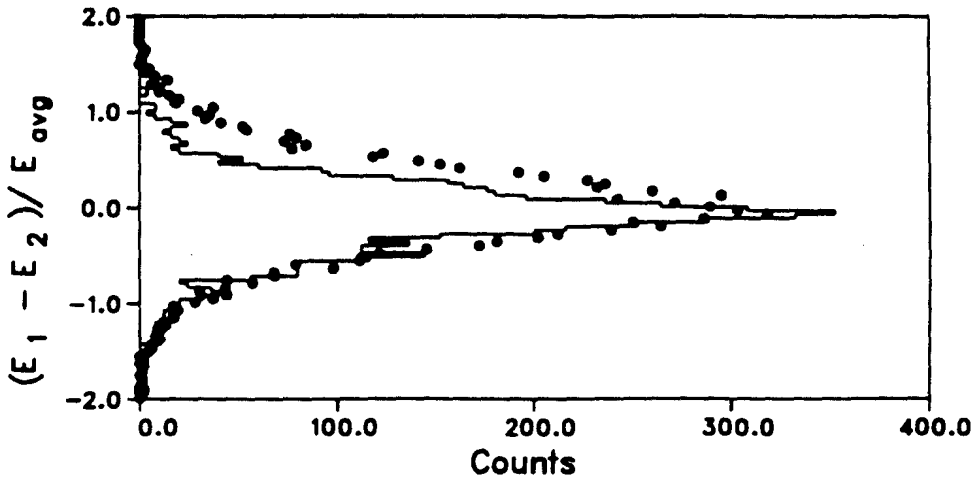


Figure 1: Relative fluctuations between energy reconstructed by FEI and FEII. Dots events below 2×10^{18} eV. Solid line : events above 2×10^{18} eV (the counts are scaled by a factor of 8 for the comparison).

FE I and FE II $(E_1 - E_2) / E_{\text{average}}$ for two energy ranges. Here E_1 is the energy as measured from Fly's Eye I information only and E_2 from Fly's Eye II. The systematic shift between Fly's Eye I and II is about 2.5%. This number shows that we have very good relative energy calibration control over the entire running period. The distribution has a standard deviation of 0.47 for events below 2×10^{18} eV and 0.40 for events above. The resulting stereo energy resolutions are 247 and 20% respectively. The uncertainty in the scintillation efficiency in air accounts to systematic error of 20%.

4. ENERGY SPECTRUM

The Fly's Eye began collecting stereo data in Nov. 1986. With two eyes observing the track simultaneously, the stereo events have much better geometrical resolution and hence energy resolution. For the data presented below, an 100% energy resolution cut has been imposed. This cut eliminates only a few poorly reconstructed events. By requiring that both eyes observe the same events, the stereo aperture is essentially the

overlapping part of the apertures of the two individual eyes. Figure 2 shows the monte carlo modeled detector exposure as a function of energy. Shown in Fig.3 is the energy spectrum derived from the number of events observed and the exposure in Fig.2. The spectrum becomes steeper right after $10^{17.6}$ eV and flattens after 3×10^{18} eV. The change in the spectral slope forms a dip where minimum lies between 2×10^{18} to 5×10^{19} eV. We divided our stereo energy spectrum into three energy ranges determined by eye and fit them to a power law spectrum in each region. Table 1 shows the normalization and the slope within each region. Also listed in Table 1 is the overall fit regardless of the details of the spectrum, though the overall spectrum does not resemble a single power law. In this paper, all the fits were done with the weighted least square method. The overall fit is dominated by the low energy points, with minor contributions from the points above 10^{19} eV. To show the significance of the dip, the numbers of events expected from the overall fit (renormalized to the observed number of events at $10^{17.6}$ eV) are listed in Table 2 with the observed numbers of events. The expected number of events between $10^{17.6}$ eV and $10^{19.6}$ eV is 5936.3, and the observed is 5477. The significance of this deficit is 5.96 σ . The chance probability of observing a dip like this with the spectrum maintains the same slope over the whole energy range is about 1.4×10^{-9} . An alternative way of showing the significance of the dip is to show the excess of the observed events above $10^{18.5}$ eV. Here we use the normalization and slope from a total fit up to $10^{18.5}$ eV to calculate the expectation. The total observed events is 283 while the expectation is 230, the excess is 3.490. Figure 1 shows that the energy resolution over this region is approximately constant, hence the spectral break is not produced by the resolution effects.

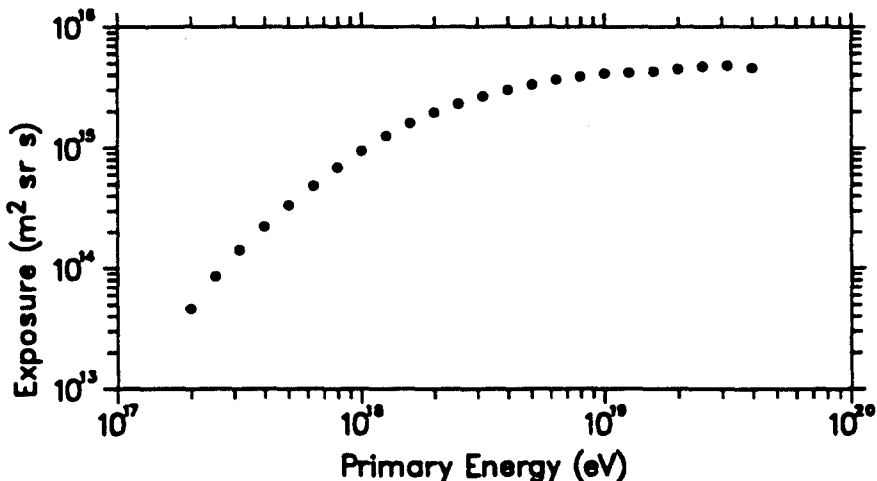


Figure2: Fly's Eye stereo exposure

Table 1. Normalizations and spectral slopes of J (E)

Energy range (eV)	power index	log(normalization)	normalized at
$10^{17.3}$ - $10^{19.6}$	-3.18 ± 0.01	-29.593	10^{18} eV
$10^{17.3}$ - $10^{17.6}$	-3.01 ± 0.06	-29.495	10^{18} eV
$10^{17.6}$ - $10^{18.5}$	-3.27 ± 0.02	-29.605	10^{18} eV
$10^{18.5}$ - $10^{19.6}$	-2.71 ± 0.10	-32.623	10^{19} eV

5. CONCLUSION

We have clearly observed a change in spectral index occurring between 2×10^{18} and 5×10^{18} eV. The spectral slopes before and after the break are -3.27 ± 0.02 and -2.71 ± 0.10 respectively.

Table 2. Number of events expected and observed

Energy bin log ₁₀ (E(eV))	# of events expected from overall fit	# of events observed	excess in a from overall fit
17.6	1050.00	1050	0.00
17.7	961.03	902	-1.90
17.8	849.45	761	-3.03
17.9	725.98	658	-2.52
18.0	601.95	571	-1.26
18.1	484.27	416	-3.10
18.2	375.63	344	-1.63
18.3	278.65	229	-2.97
18.4	198.43	162	-2.59
18.5	137.79	101	-3.13
18.6	94.17	89	-0.53
18.7	63.44	51	-1.56
18.8	42.02	43	0.15
18.9	27.30	31	0.71
19.0	17.35	21	0.88
19.1	28.35	46	3.31

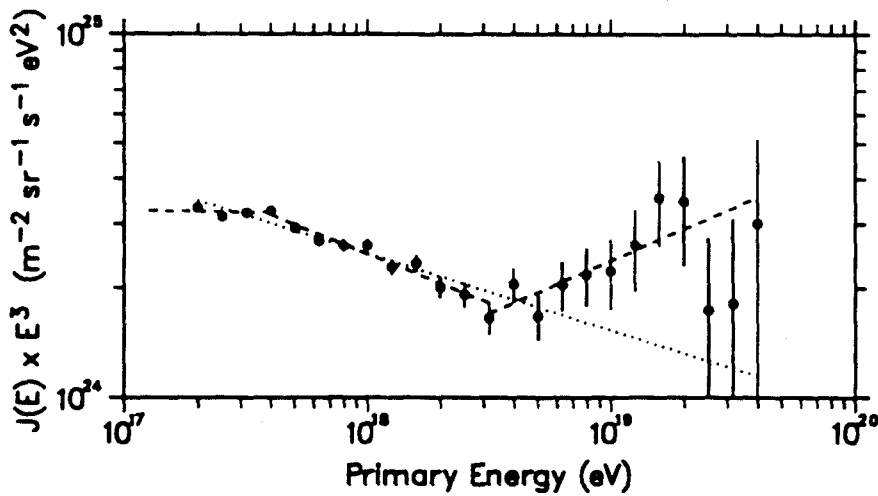


Figure 3: Fly's Eye stereo energy spectrum. Points: data. Dashed line: best fit in each region. Dotted line: best fit below $10^{18.5}$ eV.

ACKNOWLEDGEMENTS

We are indebted to Colonels Frank Cox and James King and the staff of the Dugway Proving Grounds for their continued cooperation and assistance. This work has been supported in part by the National Science Foundation (grants PHY-91-00221 at Utah and the U.S. Department of Energy (grant FG02-91 ER40677 at Illinois).

REFERENCES

- Baltrusaitis, R.M., *et al.*: 1985, Nucl. Instr. Meth. A240, 410 Efimov N. N. *et al.* 1991, Proc. Int. Symp. on Astrophysical Aspects of the Most Energetic Cosmic Rays, ed by M. Nagano and F. Takahara (Singapore World Scientific), p.20
 Lawrence, M.A., *et al.*: 1991, J. Phys. G: Nucl. Part. Phys. 17, 733 Nagano, M., *et al.*: 1992, J. Phys. G: Nucl. Part. Phys. 18, 423